

pH-Dependence of the aqueous electrochemistry of the two-electron reduced α -[Mo₁₈O₅₄(SO₃)₂] sulfite Dawson-like polyoxometalate anion derived from its triethanolammonium salt

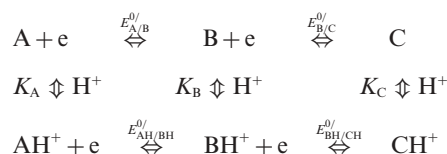
Carole Baffert,^a Stephen W. Feldberg,^a Alan M. Bond,^{*a} De-Liang Long^b and Leroy Cronin^{*b}

Received 20th April 2007, Accepted 14th June 2007

First published as an Advance Article on the web 16th August 2007

DOI: 10.1039/b705991d

The electrochemistry of the Dawson-like sulfite polyoxometalate anion α -[Mo₁₈O₅₄(SO₃)₂]⁶⁻, derived from the TEAH₆{ α -[Mo₁₈O₅₄(SO₃)₂]} salt (TEAH⁺ is the triethanolammonium cation; pK_a = 7.8), has been investigated in aqueous media using cyclic and rotated disk voltammetry at glassy carbon electrodes and bulk electrolysis, with a focus on the pH-dependence for oxidation to α -[Mo₁₈O₅₄(SO₃)₂]⁴⁻. In buffered media at pH \geq 4, the cyclic voltammetric response for α -[Mo₁₈O₅₄(SO₃)₂]⁶⁻ reveals two partially resolved one-electron oxidation processes corresponding to the sequential generation of α -[Mo₁₈O₅₄(SO₃)₂]⁵⁻ and α -[Mo₁₈O₅₄(SO₃)₂]⁴⁻. At lower pH, using electrolytes containing sulfuric acid, the two waves coalesce but the individual apparent E° reversible formal potential values for the two processes can be extracted down to pH 2 by assuming that reversible protonation accompanies fast electron transfer. The results for 2 \leq pH \leq 8 are well described by the double-square scheme mechanism:



where A, B and C correspond to species α -[Mo₁₈O₅₄(SO₃)₂]⁴⁻, α -[Mo₁₈O₅₄(SO₃)₂]⁵⁻ and α -[Mo₁₈O₅₄(SO₃)₂]⁶⁻ respectively. The following thermodynamic values could be deduced: $E_{A/B}^{\circ} = -0.009$ V vs. Fc⁺/Fc; $E_{B/C}^{\circ} = -0.125$ V vs. Fc⁺/Fc and $K_C = 1.5 \times 10^{-5}$ M; values for K_A , K_B , $E_{AH/BH}^{\circ}$ and $E_{BH/CH}^{\circ}$ could not be determined. Protonated α -[HMo₁₈O₅₄(SO₃)₂]⁵⁻, deduced to be the major species present at pH < 4, is highly stable in aqueous media. In contrast, α -[Mo₁₈O₅₄(SO₃)₂]⁶⁻, which is dominant at higher pH values, slowly decomposes. Data considered in the context of acid–base properties of both the TEAH⁺ cation and α -[HMo₁₈O₅₄(SO₃)₂]⁵⁻ anion imply that the TEAH⁺ cation is important in the isolation of (TEAH)₆{ α -[Mo₁₈O₅₄(SO₃)₂]}₆. Cyclic and rotating disk electrode voltammetries demonstrate that at least 8 electrons also can be easily added to the [Mo₁₈O₅₄(SO₃)₂]⁴⁻ framework in acidic media. The existence of the electron transfer series α -[Mo₁₈O₅₄(SO₃)₂]^{4-/5-/6-/7-/8-} was confirmed by cyclic voltammetric studies of water insoluble [Pn₄N]₄{ α -[Mo₁₈O₅₄(SO₃)₂]} adhered to a glassy carbon electrode in contact with an aqueous 0.1 M Et₄NCl electrolyte.

Introduction

Polyoxometalates have been extensively studied over the last few decades because of their relevance to catalysis,^{1–5} medicinal chemistry^{6–8} and materials science.^{9–14} The Dawson polyoxometalate structural type ([M₁₈O₅₄(XO₄)₂]ⁿ⁻; M = Mo, W and X = P, S, or Cl etc.) was first discovered over fifty years ago. Conventionally, the Dawson structure incorporates two tetrahedral anions such as PO₄³⁻,^{15,16} AsO₄³⁻,¹⁷ SO₄²⁻^{18–20} or ClO₄⁻^{21,22} within the framework structure. Recently, a new class of 18-molybdosulfite Dawson-like cluster [Mo₁₈O₅₄(SO₃)₂]⁴⁻ was isolated in both α and

β isomeric forms²³ as tetraalkylammonium salts. This molybdosulfite framework provides rich electrochemical behaviour in aprotic acetonitrile.²⁴ For example: at least 6 electrons may be added reversibly; the β isomeric configuration is retained on the voltammetric timescale upon one and two-electron reduction to the [Mo₁₈O₅₄(SO₃)₂]⁵⁻ and [Mo₁₈O₅₄(SO₃)₂]⁶⁻ anionic forms respectively; the α -isomer is slightly easier to reduce than the β form; on the much longer bulk electrolysis timescale, $\beta \rightarrow \alpha$ isomerisation occurs showing that the reduced forms of the α -isomer are thermodynamically favored over the β forms.

The redox properties of Dawson polyoxometalates in aqueous media have received limited attention²⁵ because of their low solubility and also because of their instability under basic conditions. However, it is known that the electrochemical behaviour of the sulfate polyoxometalate, [Mo₁₈O₅₄(SO₄)₂]⁴⁻, in the mixed solvent medium 95 : 5% CH₃CN–H₂O,²⁶ exhibits a large dependence

^aSchool of Chemistry, Monash University, Clayton, Victoria 3800, Australia. E-mail: alan.bond@sci.monash.edu.au

^bWestCHEM, Department of Chemistry, The University of Glasgow, Glasgow, UK G128QQ. E-mail: L.Cronin@chem.gla.ac.uk

on the hydrogen ion concentration. Reduction by two or more electrons produces highly basic forms that have been isolated as protonated polyoxometalate salts.²⁶ In the case of the sulfite class of Dawson-like polyoxometalates, a water soluble two-electron reduced α isomeric form²³ has been isolated from acidic media and characterized by X-ray crystallography as non-protonated, with respect to the polyoxometalate framework, triethanolammonium (TEAH⁺ = [HN(CH₂CH₂OH)₃]⁺) salt [TEAH]₆[Mo₁₈O₅₄(SO₃)₂]. This result suggests that the α -[Mo₁₈O₅₄(SO₃)₂]⁶⁻ anion may be significantly less basic than its sulfate analog, α -[Mo₁₈O₅₄(SO₄)₂]⁶⁻, although TEAH⁺ is a potentially non-innocent counter cation with a pK_a value of 7.8,²⁷ which may need to be taken into account.

On the basis of data reported²⁴ for the voltammetric reduction of α -[Mo₁₈O₅₄(SO₃)₂]⁴⁻ in aprotic CH₃CN, two one-electron oxidation processes to sequentially generate α -[Mo₁₈O₅₄(SO₃)₂]⁵⁻ and α -[Mo₁₈O₅₄(SO₃)₂]⁴⁻ would be expected in water as well as an additional series of reduction processes. We report here the results of voltammetric and bulk oxidative electrolysis studies of α -[Mo₁₈O₅₄(SO₃)₂]⁶⁻ derived by dissolution of the TEAH⁺ salt in buffered and non-buffered aqueous solutions. We also describe the oxidative voltammetry of (Pn₄N)₄{ α -[Mo₁₈O₅₄(SO₃)₂]} adhered to a glassy carbon electrode in contact with 0.1 M Et₄NCl aqueous electrolyte. These studies establish the pH-dependence of the redox chemistry of the sulfite Dawson polyoxometalate system in aqueous media, and also suggest the possibly special role that the TEAH⁺ cation may play in isolation of solid (TEAH)₆{ α -[Mo₁₈O₅₄(SO₃)₂]} from aqueous solutions.

To simplify the theoretical presentation of the aqueous redox chemistry of the molybdenum sulfite polyoxometalate system, we denote that A, B and C correspond to species α -[Mo₁₈O₅₄(SO₃)₂]⁴⁻, α -[Mo₁₈O₅₄(SO₃)₂]⁵⁻ and α -[Mo₁₈O₅₄(SO₃)₂]⁶⁻ respectively, and omit the α isomeric notation in most of the subsequent discussion.

Experimental

(TEAH)₆{ α -[Mo₁₈O₅₄(SO₃)₂]}·4H₂O and (Pn₄N)₄{ α -[Mo₁₈O₅₄(SO₃)₂]} were synthesized according to published procedures.²³

Doubly distilled water was used to prepare all aqueous solutions. For electrochemical studies, dioxygen was removed by purging aqueous solutions with nitrogen for at least 10 minutes. Na₂SO₄, Et₄NCl (both BDH) and H₂SO₄ (Univar) were used as electrolytes. The 0.1 M acetate buffer systems were prepared by adding 2.4 mL of a 0.1 M sodium acetate solution to 7.6 mL of a 0.1 M acetic acid solution. The required amount of solid Na₂SO₄ was then added (thereby effecting a 0.20 M Na₂SO₄ solution) along with the desired amount of (TEAH)₆[Mo₁₈O₅₄(SO₃)₂]. Phosphate buffer systems, 0.1 M, were prepared similarly by adding 1.1 mL of a 0.1 M potassium dihydrogen phosphate solution to 8.9 mL of a 0.1 M di-sodium hydrogen phosphate solution again adding the desired amount of solid Na₂SO₄ and (TEAH)₆[Mo₁₈O₅₄(SO₃)₂]. The pH of buffered solutions was adjusted upwards by addition of small aliquots of a concentrated 0.1 M KOH (BDH) solution. Dilution effects associated with the small volume changes that accompany this step were neglected. When H₂SO₄ was used as an electrolyte, 0.2 M Na₂SO₄ also was present to provide approximately constant Na⁺ concentrations for all solutions. The electrolyte solutions thus prepared represent a compromise between achieving constant ionic strength and a constant level of ion pairing.

All electrochemical experiments were undertaken at (20 ± 2 °C) with a BAS 100A electrochemical workstation (Bioanalytical Systems, West Lafayette, IN) using a standard three-electrode cell configuration with an uncompensated resistance of 400 ± 100 ohm. For cyclic voltammetry, the working electrode was a 1.5 mm diameter glassy carbon disk (Cypress Systems), the auxiliary electrode was a 1 mm diameter Pt wire, and the reference electrode was Ag/AgCl (aqueous saturated KCl, E⁰ = 0.197 V vs. SHE.²⁸ To facilitate comparisons with nonaqueous acetonitrile data, all potential values are referred to the ferricenium/ferrocene (Fc⁺/Fc couple, E⁰ = 0.400 V vs. SHE at T = 25 °C.²⁹ This procedure contains an inherent assumption that the potential of the Fc⁺/Fc couple is completely solvent independent, a scenario that is unlikely to hold exactly when comparing acetonitrile and water. We assume that the values of E⁰ for the Fc⁺/Fc couple at 20 °C and 25 °C are virtually identical.

Rotating disc electrode experiments used a 3 mm diameter GC disc working electrode (Metrohm), and a variable speed rotator (Metrohm 628–10), with auxiliary and reference electrodes the same as for cyclic voltammetry. In the case of bulk electrolysis experiments, the working electrode was carbon felt (1 × 1 × 0.2 cm), the reference electrode was Ag/AgCl (aqueous saturated KCl) and the auxiliary electrode consisted of a platinum wire isolated from the test solution by a medium porosity frit. During the course of bulk electrolysis experiments, the working electrode was held at the appropriate potential and the solution was stirred vigorously *via* nitrogen bubbling. The electrolysis was stopped when the current achieved a value that was 1% of the initial current. The procedure for mechanically adhering the solid state compound onto an electrode surface has been described in detail elsewhere.³⁰ In the present work, a small amount of solid was placed on weighing paper and the glassy carbon working electrode surface was pressed onto the solid thereby effecting adherence of the solid to the electrode. The modified electrode was then directly placed in contact with electrolyte solution. Prior to each electrochemical experiment, working electrodes were polished with a 0.05 μm Al₂O₃ (Buehler) slurry, washed with water and dried with tissue paper.

pH-Measurements were undertaken with a pH-meter (Metrohm Ion Analysis, model 744) and a pH-electrode (Metrohm 6.2306.020), whose responses were calibrated in the usual manner using standard buffer solutions. Simulations were carried out using DigiElch (available through <http://www.digielch.de/>).

Results and discussion

Electrochemical oxidation of (TEAH)₆[Mo₁₈O₅₄(SO₃)₂]}·4H₂O in aqueous media

Voltammograms of (TEAH)₆[Mo₁₈O₅₄(SO₃)₂]} dissolved in aqueous electrolyte media with pH ≤ 4 indicate that the polyoxometalate anion is stable under these conditions. In contrast, at pH > 4, instability of [Mo₁₈O₅₄(SO₃)₂]⁶⁻ is detected, as faradaic currents decrease slowly with time. Thus, our initial voltammetric studies emphasize pH ≤ 4 conditions. The cyclic voltammetric response shown in Fig. 1A was obtained for 0.98 mM (TEAH)₆[Mo₁₈O₅₄(SO₃)₂]} in unbuffered aqueous 0.2 M Na₂SO₄ (pH 3.05) at a glassy carbon electrode (scan rate = 100 mV s⁻¹) initially scanned in the positive direction from a starting potential

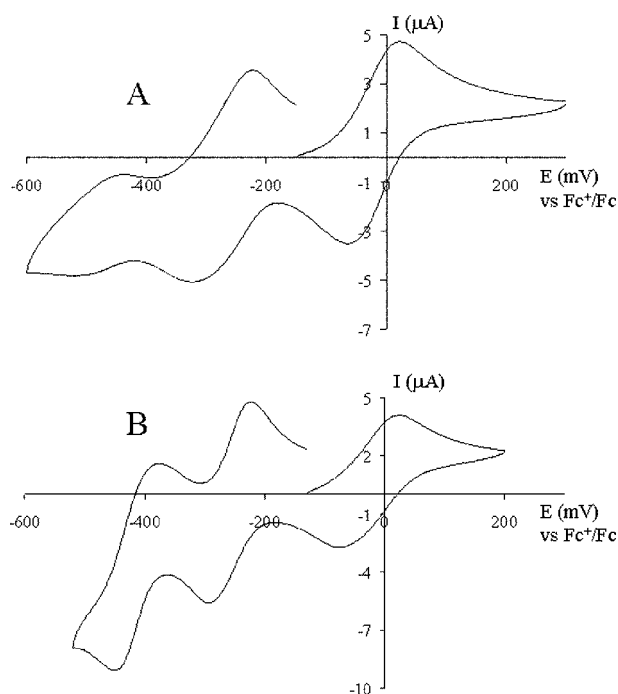


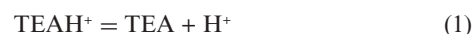
Fig. 1 Cyclic voltammograms obtained for $(\text{TEAH})_6[\text{Mo}_{18}\text{O}_{54}(\text{SO}_3)_2]$ at a GC electrode ($d = 1.5$ mm) (A) 0.980 mM solution in unbuffered 0.2 M Na_2SO_4 electrolyte; (B) 0.980 mM solution in acetate buffer/0.2 M Na_2SO_4 (pH 4). $\nu = 100$ mV s^{-1} .

of -0.15 V (chosen because it is close to the open circuit potential). The first oxidation process has a peak current of $(4.5 \pm 0.1) \times 10^{-6}$ A at ~ 0.015 V and a corresponding reduction component with a similar peak current magnitude and a peak potential at ~ -0.06 V (as noted in the experimental section, all potentials are reported vs. the Fc^+/Fc couple). The peak-to-peak separation (ΔE_p) is ~ 75 mV, with a midpoint potential (average of oxidation and reduction peak potentials) of -0.025 V. At more positive potentials, the voltammogram exhibits an irreversible process with a peak potential at 0.480 V, not shown in Fig. 1A, which is associated with oxidation of the $(\text{TEAH})^+$ cation. Two reduction processes (see later discussion) also are present with mid-point potentials of -0.275 and -0.460 V vs. Fc^+/Fc (Fig. 1A).

While the ΔE_p value of 0.075 V for the oxidation process of interest suggests a quasireversible one-electron process (the theoretical value of ΔE_p for a reversible electron transfer is about 0.056 V), a plethora of other evidence suggests that the response is a manifestation of two strongly overlapping one-electron transfers. If we assume that the diffusion coefficient of $[\text{Mo}_{18}\text{O}_{54}(\text{SO}_3)_2]^{6-}$ is 2.96×10^{-6} $\text{cm}^2 \text{ s}^{-1}$, the value measured for the comparably

sized $\alpha_2\text{-Fe}^{\text{III}}(\text{OH})_2\text{P}_2\text{W}_{17}\text{O}_{61}$ under virtually identical experimental conditions,³¹ the predicted peak current computed using DigiElch simulation software is 2.58×10^{-6} A, which is approximately half the value of the peak current observed for the oxidation process of interest in Fig. 1A. The assignment of a two-electron oxidation process also is supported by bulk electrolysis which indicated $n = 2.3$ as deduced by coulometry. The product $[\text{Mo}_{18}\text{O}_{54}(\text{SO}_3)_2]^{4-}$ (see evidence provided later) is formed with a $50 \pm 5\%$ yield on the basis of limiting currents in RDE voltammograms obtained before and after bulk electrolysis. Thus, instability of the product $[\text{Mo}_{18}\text{O}_{54}(\text{SO}_3)_2]^{4-}$ under these non-buffered conditions is detected on the long timescale (tens of minutes) of bulk electrolysis experiments, but not on the much shorter timescale (seconds) associated with voltammetric conditions.

The acidic pH 3.95 produced by a 1 mM solution of $(\text{TEAH})_6[\text{Mo}_{18}\text{O}_{54}(\text{SO}_3)_2]$ in 0.2 M Na_2SO_4 is intriguing, as it cannot solely be a consequence of the equilibrium reaction $\text{TEAH}^+ + \text{H}_2\text{O} \rightleftharpoons \text{TEAHOH} + \text{H}^+$ ($\text{p}K_a = 7.8$) effected by the reaction



A $\text{p}K_a$ value of 7.8²⁷ would produce a pH of ~ 5 . Implications of this observation will be considered later in the text.

With a 0.1 M $\text{H}_2\text{SO}_4/0.2$ M Na_2SO_4 electrolyte (pH = 0.78), a chemically reversible oxidation process (midpoint potential = 0.110 V) is detected (Fig. 2, Table 1). The ΔE_p value of 40 mV and bulk electrolysis experiments with coulometric monitoring ($n = 2.0 \pm 0.1$) demonstrate that the oxidation process at pH = 0.78 is an overall chemically reversible two-electron process in highly acidic media. Under these conditions, $[\text{Mo}_{18}\text{O}_{54}(\text{SO}_3)_2]^{4-}$ is formed by a two-electron oxidative electrolysis at close to 100% yield (RDE evidence). We also note that two sequential reversible one-electron

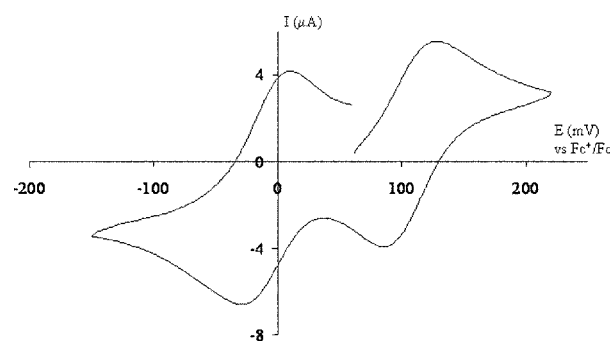


Fig. 2 Cyclic voltammograms obtained for a 1.07 mM $(\text{TEAH})_6[\text{Mo}_{18}\text{O}_{54}(\text{SO}_3)_2]$ solution at a GC electrode ($d = 1.5$ mm) in 0.1 M $\text{H}_2\text{SO}_4/0.2$ M Na_2SO_4 electrolyte. $\nu = 100$ mV s^{-1} .

Table 1 pH-Dependence of reversible potentials obtained for the overall $2e^-$ oxidation of $(\text{TEAH})_6[\text{Mo}_{18}\text{O}_{54}(\text{SO}_3)_2]$ in non-buffered aqueous media at a GC electrode. $\nu = 100$ mV s^{-1}

pH, Medium	Observed values (V) $E^{0/b}(\Delta E_p)$	Deconvoluted values (V) $E^{0/}$	
3.95, 0.2 M Na_2SO_4	-0.025 (0.075)	-0.035	-0.010
2.91, 0.001M H_2SO_4^a	-0.010 (0.045)	-0.010	-0.010
1.95; 0.01 M H_2SO_4^a	0.015 (0.040)	0.035	0.000
0.78; 0.1 M H_2SO_4^a	0.110 (0.040)	—	—

^a 0.2M Na_2SO_4 also present. ^b vs. Fc^+/Fc .

transfers with identical $E^{0'}$ values would display a ΔE_p value of 40 mV.

The electrochemistry of $(\text{TEAH})_6[\text{Mo}_{18}\text{O}_{54}(\text{SO}_3)_2]$ was also studied in 0.1 M acetate buffer at pH 4 with 0.2 M Na_2SO_4 also present, as with other solutions. The cyclic voltammetry of $(\text{TEAH})_6[\text{Mo}_{18}\text{O}_{54}(\text{SO}_3)_2]$ under these buffered conditions at a glassy carbon electrode at a scan rate of 100 mV s^{-1} exhibits similar behavior to that observed in aqueous non-buffered 0.2 M Na_2SO_4 electrolyte. Thus, a reversible oxidation process is detected (Fig. 1B) with a midpoint potential of -0.030 V (Table 2), which is again followed by an irreversible TEAH^+ oxidation process at 0.500 V. Two reversible reduction processes are also again detected (Fig. 1B) with mid-point potentials of -0.265 V and -0.415 V . Oxidative bulk electrolysis of $[\text{Mo}_{18}\text{O}_{54}(\text{SO}_3)_2]^{6-}$ at 0.100 V leads to the formation of $[\text{Mo}_{18}\text{O}_{54}(\text{SO}_3)_2]^{4-}$ species with a reasonably high yield ($>80\%$). Coulometric data ($n = 2.0 \pm 0.1$) derived from this experiment is in excellent agreement with the postulated overall two-electron oxidation process.

When the pH value is increased under buffered conditions to the value of 5, the overall two-electron oxidation process assumed to be present under more acidic conditions splits into two closely spaced partially resolved processes (Fig. 3A and B). As the pH value is increased further (up to pH 8), the midpoint potential of the (second) more positive oxidation process remains almost independent of pH. In contrast, the potential of the more negative (first) process shifts in the negative potential direction (Fig. 4, Table 2), so that the two processes eventually become almost fully resolved at higher pH values. In basic phosphate buffer at pH 8, the two chemically and almost electrochemically reversible processes expected on the basis of studies in CH_3CN are observed with midpoint or reversible formal potential $E^{0'}$ values of -0.140 and -0.010 V (Fig. 3C, Table 2), and ΔE_p -values of around 70 mV. The irreversible TEAH^+ cation oxidation process exhibits a peak at 0.510 V. However, at this pH value $[\text{Mo}_{18}\text{O}_{54}(\text{SO}_3)_2]^{6-}$, $[\text{Mo}_{18}\text{O}_{54}(\text{SO}_3)_2]^{5-}$ and the fully oxidized $[\text{Mo}_{18}\text{O}_{54}(\text{SO}_3)_2]^{4-}$ (the latter two generated by bulk electrolysis) are all unstable, as evidenced by time dependent RDE voltammetry.

Rotating disk electrode experiments confirm the attribution of two one-electron processes at $\text{pH} \geq 6$ where two resolved

Table 2 pH-Dependence of reversible potentials obtained for the two-electron oxidation of $(\text{TEAH})_6[\text{Mo}_{18}\text{O}_{54}(\text{SO}_3)_2]$ in buffered (0.2 M Na_2SO_4) aqueous media at GC electrode. pH 8 to 6 (0.1 M phosphate buffer). pH 5.5 to 4 (0.1 M acetate buffer). $\nu = 100 \text{ mV s}^{-1}$

pH	$E^{0'}/\alpha(\Delta E_p)$ (V) for	
	$[\text{Mo}_{18}\text{O}_{54}(\text{SO}_3)_2]^{6-/5-}$	$[\text{Mo}_{18}\text{O}_{54}(\text{SO}_3)_2]^{5-/4-}$
8.00	-0.140 (0.070)	-0.010 (0.065)
7.55	-0.125 (0.070)	-0.005 (0.080)
7.00	-0.125 (0.070)	-0.010 (0.075)
6.50	-0.125 (0.080)	-0.010 (0.075)
6.00	-0.125 (0.065)	-0.010 (0.065)
5.50	-0.110 (0.065)	-0.005 (0.065)
5.05	-0.095 (0.060)	-0.005 (0.055)
4.50	-0.050 (0.100) ^b	
	-0.100^c	0.020^c
4.00	-0.030 (0.080) ^b	
	-0.075^c	-0.015^c

^a vs. Fc^+/Fc . ^b Midpoint potential and peak separation of composite wave. ^c Values obtained after deconvolution.

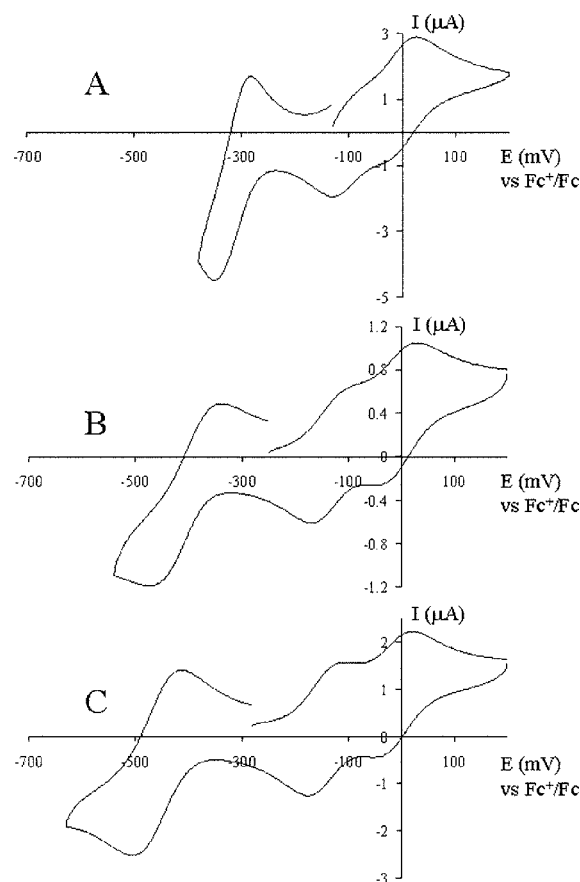


Fig. 3 Cyclic voltammograms obtained for $(\text{TEAH})_6[\text{Mo}_{18}\text{O}_{54}(\text{SO}_3)_2]$ at a GC electrode ($d = 1.5 \text{ mm}$): (A) 0.98 mM solution in aqueous acetate buffer/0.2 M Na_2SO_4 (pH 5.05); (B) a 0.98 mM solution in acetate buffer/0.2 M Na_2SO_4 (pH 6); (C) 0.98 mM solution in phosphate buffer/0.2 M Na_2SO_4 (pH 8). $\nu = 100 \text{ mV s}^{-1}$.

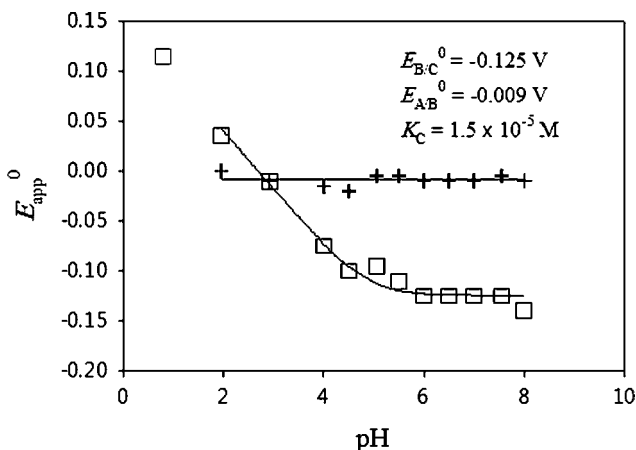


Fig. 4 Plots of reversible $E^{0'}$ potentials for the oxidation of $(\text{TEAH})_6[\text{Mo}_{18}\text{O}_{54}(\text{SO}_3)_2]$ as a function of pH (\square : $[\text{Mo}_{18}\text{O}_{54}(\text{SO}_3)_2]^{5-/6-}$ couple; $+$: $[\text{Mo}_{18}\text{O}_{54}(\text{SO}_3)_2]^{4-/5-}$ couple). Value (\square) given at pH 7.8 is the mid-point potential detected experimentally, and not a deconvoluted $E^{0'}$ value.

oxidation waves are detected with limiting current ratios close to 1 : 1 (Fig. 5). The diffusion coefficient calculated *via* use of the Levich equation at pH 4 was $3 \times 10^{-6} \text{ cm}^2 \text{ s}^{-1}$ and similar to values reported for polyoxometalate compounds^{24,31} of

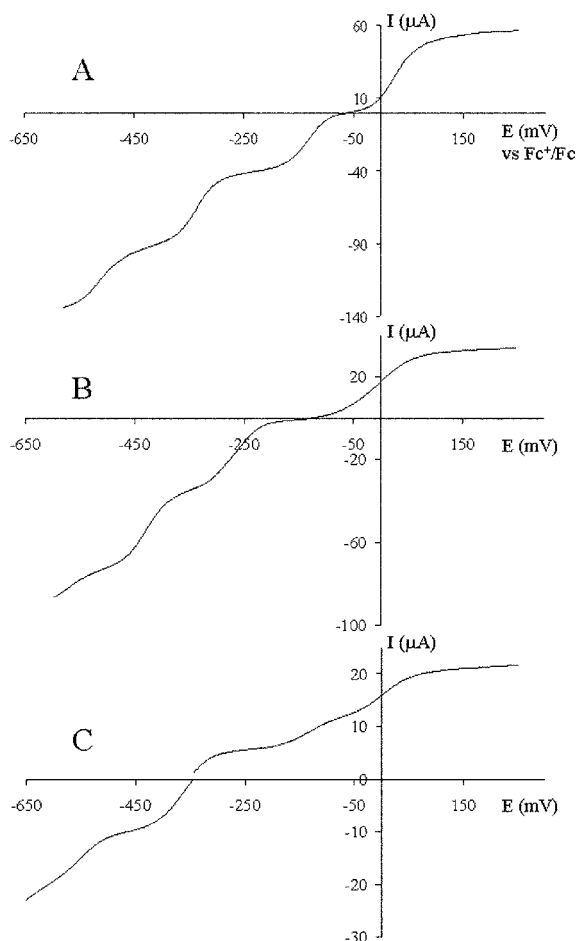
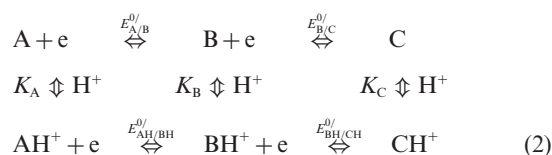


Fig. 5 Rotating disc voltammograms at a GC ($d = 3$ mm) electrode ($v = 10$ mV s^{-1} , $\omega = 2000$ rpm) obtained for (TEAH)₆[Mo₁₈O₃₄(SO₃)₂] (A) 0.967 mM solution in 0.01 M H₂SO₄/0.2 M Na₂SO₄; (B) 0.98 mM solution in acetate buffer/0.2 M Na₂SO₄ at pH 4; (C) 0.98 mM solution in phosphate buffer/0.2 M Na₂SO₄ at pH 6.

similar charge and molecular weight. The progressively smaller magnitude of the limiting current value for the overall two-electron oxidation process per unit concentration as the pH value is increased is attributed to decomposition of [Mo₁₈O₃₄(SO₃)₂]⁶⁻ which becomes most notable at pH ≥ 5 . Interestingly, at pH ≥ 6 , the potential of zero-current is not in the expected position. That is, the first formerly reduction wave (Fig. 5C) now has partially oxidative character indicating that the instability of [Mo₁₈O₃₄(SO₃)₂]⁶⁻ may be associated with formation of a reduced form of [Mo₁₈O₃₄(SO₃)₂]⁶⁻ and another product(s) *via* an unknown mechanism.

On the basis of the pH-dependence of the voltammetry, we propose that the oxidation of [Mo₁₈O₃₄(SO₃)₂]⁶⁻ on the cyclic voltammetric time scale can be described by the double square scheme:



where we have assumed that the electron transfers are reversible—experimentally observed peak separations slightly larger than would be predicted by reversible electron transfer may be attributed primarily to uncompensated resistance. The equilibrium constants are defined by

$$K_A = \frac{a_{H^+}[A]}{[AH^+]} \quad (3)$$

$$K_B = \frac{a_{H^+}[B]}{[BH^+]} \quad (4)$$

and

$$K_C = \frac{a_{H^+}[C]}{[CH^+]} \quad (5)$$

Microscopic reversibility requires

$$\begin{aligned}
 \frac{[B]}{[A]} \times \frac{[BH^+]}{[B]} \times \frac{[AH^+]}{[BH^+]} \times \frac{[A]}{[AH^+]} &= 1 \\
 &= \frac{K_A}{K_B} \exp[E_{A/B}^0 - E_{AH/BH}^0]
 \end{aligned} \quad (6)$$

and

$$\begin{aligned}
 \frac{[C]}{[B]} \times \frac{[CH^+]}{[C]} \times \frac{[BH^+]}{[CH^+]} \times \frac{[B]}{[BH^+]} &= 1 \\
 &= \frac{K_B}{K_C} \exp[E_{B/C}^0 - E_{BH/CH}^0]
 \end{aligned} \quad (7)$$

Our approach and notation follows that described previously by Guo *et al.*³¹ with the added assumption for the present system that all electron transfers are reversible. As long as the protonations accompanying electron transfer are reversible, reaction scheme (2) can be effectively represented by the EE sequence:



where $[A_{\text{eff}}] = [A] + [AH^+]$; $[B_{\text{eff}}] = [B] + [BH^+]$ and $[C_{\text{eff}}] = [C] + [CH^+]$ are functions of pH and $E_{\text{app,A/B}}^0$ and $E_{\text{app,B/C}}^0$ are functions of pH and the formal reversible potentials for the individual redox processes shown in eqn (2); for details of the derivation of the following equations see ref. 31. Then

$$\begin{aligned}
 \frac{F}{RT}(E_{\text{app,A/B}}^0 - E_{\text{AH/BH}}^0) &= \ln \left[\frac{K_B + \frac{a_{H^+}}{K_A}}{1 + \frac{a_{H^+}}{K_A}} \right] \\
 &= \ln \left[\frac{K_B + a_{H^+}}{K_A + a_{H^+}} \right] = \ln \left[\frac{K_B + 10^{-\text{pH}}}{K_A + 10^{-\text{pH}}} \right]
 \end{aligned} \quad (9)$$

and

$$\begin{aligned}
 \frac{F}{RT}(E_{\text{app,B/C}}^0 - E_{\text{BH/CH}}^0) &= \ln \left[\frac{\frac{K_C}{K_B} + \frac{a_{H^+}}{K_B}}{1 + \frac{a_{H^+}}{K_B}} \right] \\
 &= \ln \left[\frac{K_C + a_{H^+}}{K_B + a_{H^+}} \right] = \ln \left[\frac{K_C + 10^{-\text{pH}}}{K_B + 10^{-\text{pH}}} \right]
 \end{aligned} \quad (10)$$

Our first objective was to use simulations (generated with DigiElch) to deconvolve the two one-electron processes assumed to be present under conditions of cyclic voltammetry. From these deconvolutions, $E_{\text{app,A/B}}^0$ and $E_{\text{app,B/C}}^0$ can be deduced for the two

component reaction scheme (eqn (8)) over the range $2 \leq \text{pH} \leq 8$. Any apparent quasireversibility was attributed to uncompensated resistance. The $E^{0'}$ data derived over the pH range 2 to 8 are summarized in Tables 1 and 2. Eqn (9) and (10) can now be used to ascertain just which of the thermodynamic parameters in eqn (2) can be uniquely determined from the dependence of $E^{0'}$ values on pH.

A plot of $E_{\text{app,A/B}}^{0'}$ and $E_{\text{app,B/C}}^{0'}$ vs. pH is shown in Fig. 4. $E_{\text{app,A/B}}^{0'}$ is virtually independent of pH, suggesting that one of the following three conditions has been met (see eqn (9))

$$a_{\text{H}^+} \ll K_{\text{B}} \quad \text{and} \quad a_{\text{H}^+} \ll K_{\text{A}} \quad (11)$$

or

$$a_{\text{H}^+} \gg K_{\text{B}} \quad \text{and} \quad a_{\text{H}^+} \gg K_{\text{A}} \quad (12)$$

or

$$K_{\text{A}} = K_{\text{B}} \quad (13)$$

In contrast, the plot of $E_{\text{app,B/C}}^{0'}$ vs. pH exhibits a limiting slope at low pH of approximately -0.060 V/pH and then begins to flatten at higher pH. From eqn (10) we see that this result can be obtained only when

$$a_{\text{H}^+} \gg K_{\text{C}} \quad \text{and} \quad a_{\text{H}^+} \ll K_{\text{B}} \quad (14)$$

It therefore follows that:

$$K_{\text{C}} \ll K_{\text{B}} \quad (15)$$

Based on the charges (-4 , -5 and -6) on species A, B, and C, it is chemically sensible to suggest that

$$K_{\text{A}} > K_{\text{B}} > K_{\text{C}} \quad (16)$$

thereby ruling out eqn (15).

The conditions of eqn (12) and (14) are contradictory; thus the condition of eqn (12) cannot be met, thus the chemically sensible conditions of eqn (11) must obtain. Then the operative form of eqn (10) will be

$$\begin{aligned} E_{\text{app,B/C}}^{0'} &= \frac{RT}{F} \ln \left[\frac{K_{\text{C}} + 10^{-\text{pH}}}{K_{\text{B}}} \right] + E_{\text{BH/CH}}^{0'} \\ &= \frac{RT}{F} \ln [K_{\text{C}} + 10^{-\text{pH}}] + E_{\text{BH/CH}}^{0'} - \frac{RT}{F} \ln [K_{\text{B}}] \quad (17) \end{aligned}$$

In the region of high pH, this becomes

$$E_{\text{app,B/C}}^{0'} \underset{\text{limit of High pH}}{=} \frac{RT}{F} \ln \left[\frac{K_{\text{C}}}{K_{\text{B}}} \right] + E_{\text{BH/CH}}^{0'} = E_{\text{B/C}}^{0'} \quad (18)$$

The solid line through the (\square) data in Fig. 4 represents the best least-squares fit with the following optimized parameter values: $K_{\text{C}} = 1.5 \times 10^{-5} \text{ M}$ and $E_{\text{B/C}}^{0'} = -0.125 \text{ V}$. With the conditions of eqn (11), the operative form of eqn (9) becomes (with eqn (6))

$$E_{\text{app,A/B}}^{0'} = \frac{RT}{F} \ln \left[\frac{K_{\text{B}}}{K_{\text{A}}} \right] + E_{\text{AH/BH}}^{0'} = E_{\text{A/B}}^{0'} \quad (19)$$

On inspection of the (+) data in Fig. 4, we can conclude that $E_{\text{A/B}}^{0'} = 0.009 \text{ V}$.

The above analysis was based on data obtained at a scan rate of 100 mV s^{-1} . Analysis of data obtained over the scan rate range of 20 to 1000 mV s^{-1} and concentrations of $[\text{Mo}_{18}\text{O}_{54}(\text{SO}_3)_2]^{6-}$ over the range 0.5 to 1.0 mM, and using the same protocol gave

essentially identical $E^{0'}$ and K_{C} values, as would be expected when only thermodynamic parameters have been determined. The small increase of ΔE_{p} with scan rate detected is predominantly attributed to ohmic drop and not slow electron transfer—a conclusion that is consistent with measured values of the uncompensated resistance.

Simulations of the cyclic voltammetry based on features described above from the double square scheme in buffered media over the pH range of 4 to 8 (Fig. 6) using DigiElch software describe most aspects of the experimental voltammograms. Full theoretical accounts of various aspects of these square or more extended ladder schemes are available in a number of publications.³¹⁻⁴⁶ The electrode area was 0.017 cm^2 . The $E_{\text{A/B}}^{0'}$ and $E_{\text{B/C}}^{0'}$ values were as given above. Since $[\text{Mo}_{18}\text{O}_{54}(\text{SO}_3)_2]^{6-}$ is not stable at high pH, the initial concentration of $[\text{Mo}_{18}\text{O}_{54}(\text{SO}_3)_2]^{6-}$ present at the time voltammograms were recorded, was calculated

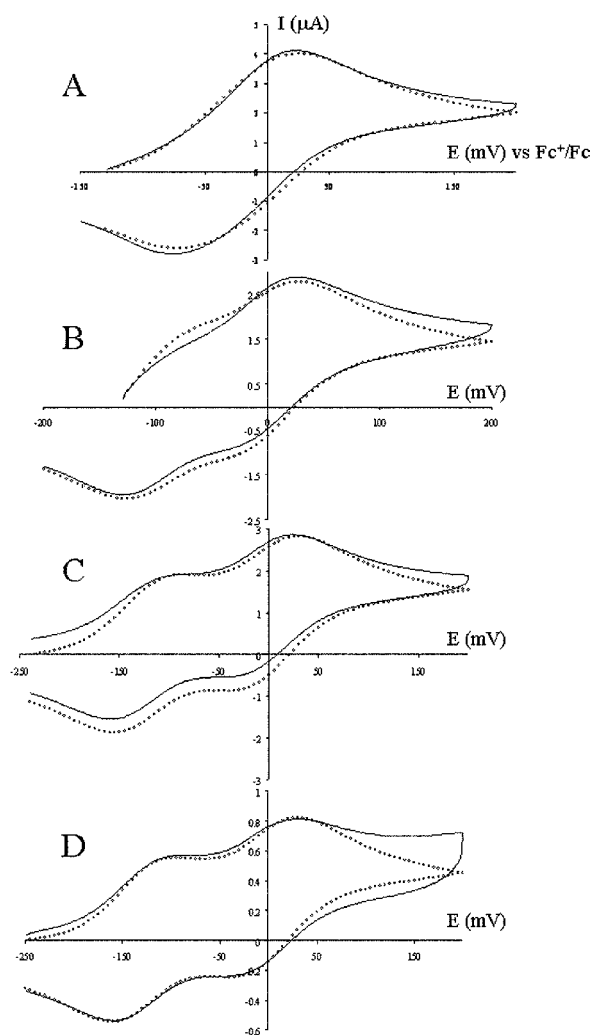


Fig. 6 Comparison of experimental (—) cyclic voltammograms ($v = 100 \text{ mV}$) obtained at a GC electrode ($d = 1.5 \text{ mm}$) for (A) 0.98 mM $(\text{TEAH})_6[\text{Mo}_{18}\text{O}_{54}(\text{SO}_3)_2]$ in acetate buffer/ $0.2 \text{ M Na}_2\text{SO}_4$ at pH 4; (B) 0.98 mM $(\text{TEAH})_6[\text{Mo}_{18}\text{O}_{54}(\text{SO}_3)_2]$; acetate buffer/ $0.2 \text{ M Na}_2\text{SO}_4$ at pH 5.05; (C) 0.98 mM $(\text{TEAH})_6[\text{Mo}_{18}\text{O}_{54}(\text{SO}_3)_2]$ in phosphate buffer/ $0.2 \text{ M Na}_2\text{SO}_4$ at pH 6; (D) 0.98 mM solution in phosphate buffer/ $0.2 \text{ M Na}_2\text{SO}_4$ at pH 7 and simulated (\cdots) cyclic voltammograms. Simulation and other experimental parameters are as stated in the text.

Table 3 Summary of reversible potentials for reduction of $(\text{Pn}_4\text{N})_4[\text{Mo}_{18}\text{O}_{54}(\text{SO}_3)_2]$ at a GC electrode. $v = 20 \text{ mV s}^{-1}$ in water acid acetonitrile

pH and/or electrolyte	$E^{0'}$ in V vs. Fc^+/Fc for $[\text{Mo}_{18}\text{O}_{54}(\text{SO}_3)_2]^{n-/(n-1)-}$			
	4-/5-	5-/6-	6-/7-	7-/8-
9.4; 0.1 M Et_4NCl in H_2O^a	-0.110	-0.215	-0.405	-0.485
0.1 M Hx_4NClO_4 in CH_3CN^b	-0.005	-0.265	-0.885	-1.195

^a Solid mechanically attached to a GC electrode in contact with aqueous electrolyte media. ^b Dissolved in CH_3CN .

from RDE data and using a diffusion coefficient of 3×10^{-6} at all pH values. It was assumed that the protonation and deprotonation reactions equilibrate on the cyclic voltammetric timescale with K_C set at 1.5×10^{-5} M and $K_A \gg K_B \gg K_C$. However, the values of K_A and K_B chosen for the simulation, and hence the $E_{\text{AH}/\text{BH}}^{0'}$ and $E_{\text{BH}/\text{CH}}^{0'}$ values derived from the chosen K values *via* the thermodynamic relationships $\Delta E^{0'} = -RT \ln K$, are not physically significant in the sense that simulations are insensitive to their value, provided $K_A \gg K_B \gg K_C$. The buffer reactions and the TEAH^+ acid–base behavior were accounted for as described in ref. 31. A value of the Butler–Volmer charge-transfer coefficient of 0.5 was used in simulations in Fig. 6 along with the standard rate constants for charge transfer, $k_{\text{AH}/\text{BH}}^{0'} = k_{\text{BH}/\text{CH}}^{0'} = 0.02 \text{ cm s}^{-1}$ and $k_{\text{A}/\text{B}}^{0'} = k_{\text{B}/\text{C}}^{0'} = 0.01 \text{ cm s}^{-1}$ (subscripts correspond to those for the standard potentials as shown in eqn (2)). However, simulations based on uncompensated resistance of 400 ± 100 ohm and reversible electron transfer kinetics were also in equally satisfactory agreement with experiment. Thus, electrode kinetics cannot be determined from these experiments.

The voltammetry for the two-electron oxidation of $[\text{Mo}_{18}\text{O}_{54}(\text{SO}_3)_2]^{6-}$ to $[\text{Mo}_{18}\text{O}_{54}(\text{SO}_3)_2]^{4-}$ in basic aqueous media is consistent with that found for the two-electron reduction of $[\text{Mo}_{18}\text{O}_{54}(\text{SO}_3)_2]^{4-}$ to $[\text{Mo}_{18}\text{O}_{54}(\text{SO}_3)_2]^{6-}$ in aprotic organic media. However, some thermodynamic differences are evident, for example: the separation in potential between the $[\text{Mo}_{18}\text{O}_{54}(\text{SO}_3)_2]^{4-/5-}$ and $[\text{Mo}_{18}\text{O}_{54}(\text{SO}_3)_2]^{5-/6-}$ processes is significantly less in water ($\Delta E^{0'} = 0.130 \text{ V}$ at pH 8, see Table 2) than in acetonitrile ($\Delta E^{0'} = 0.260 \text{ V}$, first two columns Table 3). Interestingly, assuming the approximation that the potential of the Fc^+/Fc process is independent of solvent is reasonable for CH_3CN *versus* water, the potentials for the $[\text{Mo}_{18}\text{O}_{54}(\text{SO}_3)_2]^{4-/5-}$ couple are concluded to be similar in water (buffered at pH 8) and in acetonitrile (0.1 M Hx_4NClO_4) with $E^{0'} = -0.010$ and -0.005 V vs. Fc^+/Fc , respectively. Usually, for solvent polarity reasons, reversible potentials for Dawson polyoxometalates are observed at significantly more positive values in water than in acetonitrile.^{24,27–28} In the present case, the commonly observed solvent dependence is detected in the $[\text{Mo}_{18}\text{O}_{54}(\text{SO}_3)_2]^{5-/6-}$ but not the $[\text{Mo}_{18}\text{O}_{54}(\text{SO}_3)_2]^{4-/5-}$ couples.

pH Value of $(\text{TEAH})_6[\text{Mo}_{18}\text{O}_{54}(\text{SO}_3)_2]$ dissolved in non-buffered aqueous 0.2 M Na_2SO_4 media

The pH value of ~ 4 found for 1 mM solutions of $(\text{TEAH})_6[\text{Mo}_{18}\text{O}_{54}(\text{SO}_3)_2]$ dissolved in unbuffered, degassed, 0.2 M Na_2SO_4 is intriguing. As noted above, the $\text{p}K_a$ of the TEAH^+ cation has been reported to be 7.8.²⁷ The present study has estab-

lished the K_A of $[\text{HMo}_{18}\text{O}_{54}(\text{SO}_3)_2]^{5-}$ to be 1.5×10^{-5} M. Thus, a 1 mM aqueous solution of $(\text{TEAH})_6[\text{Mo}_{18}\text{O}_{54}(\text{SO}_3)_2]$ ought have a pH ~ 5.0 because of the dissociation of the TEAH^+ ($\text{p}K_a = 7.8$). In contrast, the pH of a solution of 1 mM $(\text{TEAH})_5[\text{HMo}_{18}\text{O}_{54}(\text{SO}_3)_2]$ would be predicted to be about 4, as found experimentally. Consequently, the possibility that the putative $(\text{TEAH})_6[\text{Mo}_{18}\text{O}_{54}(\text{SO}_3)_2]$ sample contains $(\text{TEAH})_5[\text{HMo}_{18}\text{O}_{54}(\text{SO}_3)_2]$ or acidic impurities or decomposes on dissolution to give a pH value around 4 needs to be considered. The X-ray structure obtained from a single crystal isolated from the bulk synthesized material²³ has 6 well defined TEAH^+ cations, even though slight site disorder was found in the location of the sixth TEAH^+ cation. Thus, it is clear that the crystal used for the X-ray structure determination was not $(\text{TEAH})_5[\text{HMo}_{18}\text{O}_{54}(\text{SO}_3)_2]$. However, it is worth noting that the solid was prepared by reduction of MoO_4^{2-} solutions adjusted to pH 4 with hydrochloric acid. At this pH value, a significant concentration of $[\text{HMo}_{18}\text{O}_{54}(\text{SO}_3)_2]^{5-}$ would be present. Thus, it is possible that bulk solid contains both $(\text{TEAH})_6[\text{Mo}_{18}\text{O}_{54}(\text{SO}_3)_2]$ and $(\text{TEAH})_5[\text{HMo}_{18}\text{O}_{54}(\text{SO}_3)_2]$. Elemental analysis²³ based on $(\text{TEAH})_6[\text{Mo}_{18}\text{O}_{54}(\text{SO}_3)_2] \cdot 4\text{H}_2\text{O}$ produced lower C and H% than theoretically predicted, but a higher N%, so is not definitive on this matter. Furthermore, under conditions of pH ≥ 5 , where $[\text{Mo}_{18}\text{O}_{54}(\text{SO}_3)_2]^{6-}$ is the dominant species, significant decomposition of the polyoxometalate system takes place. Plausibly, decomposition by hydrolysis could produce a stable solution at about pH 4 to provide an environment where $[\text{HMo}_{18}\text{O}_{54}(\text{SO}_3)_2]^{5-}$ is stable.

Reduction of $(\text{TEAH})_6[\text{Mo}_{18}\text{O}_{54}(\text{SO}_3)_2] \cdot 4\text{H}_2\text{O}$ in aqueous media

In addition to being oxidized to $[\text{Mo}_{18}\text{O}_{54}(\text{SO}_3)_2]^{4-}$, $[\text{Mo}_{18}\text{O}_{54}(\text{SO}_3)_2]^{6-}$ also gives rise to a series of reduction processes. The mid-point potential derived from cyclic voltammograms at a glassy carbon electrode for the first reduction process shifts from -0.010 V to -0.465 V vs. Fc^+/Fc over the pH range of 0.78 to 8 (Fig. 7). Rotating disk electrode experiments in sulfuric acid media provide information on the overall number of electrons associated with this reduction process. The fact that the oxidation process in acidic media represents an overall two-electron process, and the first reduction process exhibits the same limiting current value (sign of course is different) under acidic conditions (Fig. 5A) implies that the first reduction process

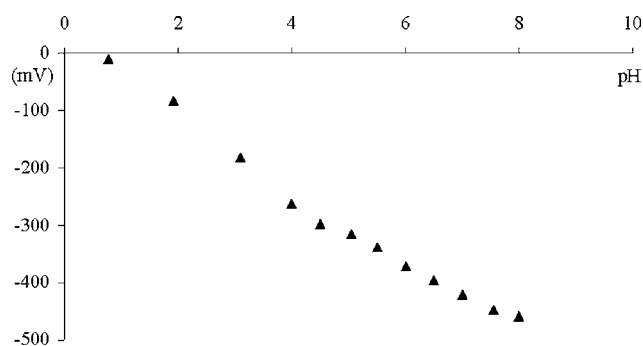
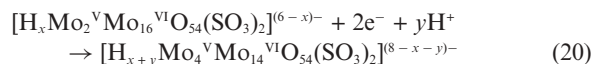


Fig. 7 Plot of mid-point potentials (values at pH 4–8 refer to buffered media, values at lower pH refer to sulfuric acid electrolyte media) as a function of pH obtained at a GC electrode for the first $(\text{TEAH})_6[\text{Mo}_{18}\text{O}_{54}(\text{SO}_3)_2]$ reduction process. $v = 100 \text{ mV s}^{-1}$.

also represents on overall two-electron process. However, in this case, insufficient information is available to establish the details of the number of protons coupled to individual electron transfer steps. Thus, only the overall reaction scheme is known:



As shown in Fig. 5A and B, two more electrons can be readily added to $[\text{H}_{x+y}\text{Mo}_4^{\text{V}}\text{Mo}_{14}^{\text{VI}}\text{O}_{54}(\text{SO}_3)_2]^{(8-x-y)-}$ to produce a four-electron reduced and even more extensively protonated polyoxometalate system. The net six-electron reduction of the $[\text{Mo}_{18}\text{O}_{54}(\text{SO}_3)_2]^{4-}$ framework thereby achieved *via* three overall two-electron steps in acidic aqueous media parallels the six one-electron charge transfer processes detected in aprotic acetonitrile.²⁴ However, very strong protonation even allows an eight-electron reduced species to be formed (Fig 5A), within the potential range available at a GC electrode in highly acidic aqueous media.

Voltammetric studies of surface confined $(\text{Pn}_4\text{N})_4[\text{Mo}_{18}\text{O}_{54}(\text{SO}_3)_2]$ in aqueous media

$[\text{Mo}_{18}\text{O}_{54}(\text{SO}_3)_2]^{4-}$, isolated as the Pn_4N^+ salt, is not soluble in water. However, voltammetric data may be obtained at pH 9.4 *via* use of the solid mechanically attached to a glassy carbon electrode in contact with water containing 0.1 M Et_4NCl as the electrolyte.⁴⁷ The cyclic voltammetry under these conditions at a scan rate of 20 mV s^{-1} now exhibits four chemically reversible one-electron reduction processes having $E^{\text{O}^{\text{I}}}$ values of -0.110 V, -0.215 V, -0.405 V and -0.485 V vs. Fc^+/Fc (Fig. 8, Table 3). Since the processes exhibit diffusion-controlled characteristics, it is assumed that exchange of the Pn_4N^+ cation with electrolyte cation Et_4N^+ occurs after the initial one-electron reduction process, which produces water soluble reduced $[\text{Mo}_{18}\text{O}_{54}(\text{SO}_3)_2]^{5-}$ according to reaction scheme

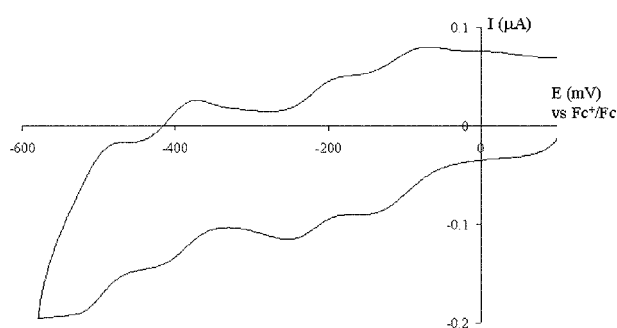
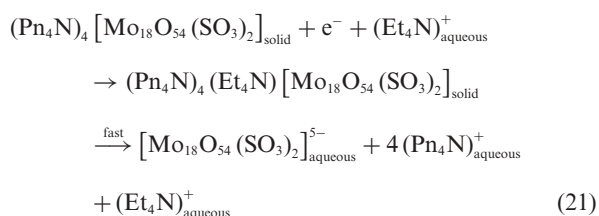
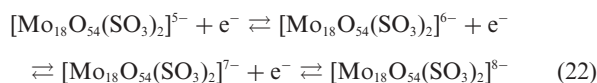


Fig. 8 Cyclic voltammogram obtained for $(\text{Pn}_4\text{N})_4[\text{Mo}_{18}\text{O}_{54}(\text{SO}_3)_2]$ as a solid adhered to a glassy carbon electrode ($d = 1.5$ mm) in contact with aqueous 0.1 M Et_4NCl electrolyte at pH 9.4. $\nu = 20$ mV s^{-1} .

This dissolution process then allows the extended solution phrase reaction scheme



to be identified. Cyclic voltammetry at pH 9.4 now parallels that obtained in aprotic acetonitrile where a series of one-electron process are detected. Again, when both data sets are converted to the Fc^+/Fc scale, the potential of the $[\text{Mo}_{18}\text{O}_{54}(\text{SO}_3)_2]^{4-/5-}$ process is found to be more negative in acetonitrile than in water. However, the usual order of reversible potentials of polyoxometalate being more positive in water is found for the $[\text{Mo}_{18}\text{O}_{54}(\text{SO}_3)_2]^{6-/7-}$ couples. It is assumed that a lower extent of ion pairing is obtained when the electrolyte cation is Et_4N^+ at a concentration of 0.1 M (instead of Na^+ at a concentration 0.4 M). This could contribute to the differences in potentials in Tables 2 and 3.

Conclusions

Voltammograms obtained from $(\text{TEAH})_6[\text{Mo}_{18}\text{O}_{54}(\text{SO}_3)_2]$ in aqueous media exhibit a strong dependence on pH. As anticipated on the basis of data available for reduction of $[\text{Mo}_{18}\text{O}_{54}(\text{SO}_3)_2]^{4-}$ in aprotic acetonitrile media, where six one-electron well resolved steps are detected, $[\text{Mo}_{18}\text{O}_{54}(\text{SO}_3)_2]^{6-}$ can be both oxidized and reduced. Thus, the expected two reversible one-electron oxidation $[\text{Mo}_{18}\text{O}_{54}(\text{SO}_3)_2]^{6-/5-}$ processes can be detected, but only at $\text{pH} \geq 5$. At lower pH values, the two processes are merged into an overall two-electron pH dependent oxidation process, as is the case in acid media with other polyoxometalates.^{48,49} The pK_a values for $[\text{HMo}_{18}\text{O}_{54}(\text{SO}_3)_2]^{6-}$ have been determined as have reversible potentials for the $[\text{Mo}_{18}\text{O}_{54}(\text{SO}_3)_2]^{6-/5-}$ and $[\text{Mo}_{18}\text{O}_{54}(\text{SO}_3)_2]^{5-/4-}$ processes. Simulations support the hypothesis that the interconversion of the $[\text{Mo}_{18}\text{O}_{54}(\text{SO}_3)_2]^{4-}$ and $[\text{Mo}_{18}\text{O}_{54}(\text{SO}_3)_2]^{6-}$ systems takes place in aqueous media *via* a double square scheme involving the reversible coupling of charge and proton transfer. $[\text{Mo}_{18}\text{O}_{54}(\text{SO}_3)_2]^{6-}$ also may be reduced in a series of overall two-electron processes. Thus, in aqueous media, at least 8 electrons can be added to the fully oxidized $[\text{Mo}_{18}\text{O}_{54}(\text{SO}_3)_2]^{4-}$ framework by a combination of coupled one-electron charge and multi-levels of proton transfer processes.

References

- I. V. Kozhevnikov, *Chem. Rev.*, 1998, **98**, 171–198.
- Catalysis by Polyoxometalates, *Catalysts for Fine Chemical Synthesis*, John Wiley and sons, Chichester, 2002, vol. 2.
- N. Mizuno and M. Misono, *Chem. Rev.*, 1998, **98**, 199–217.
- C. L. Hill, *Angew. Chem., Int. Ed.*, 2004, **43**, 402–404.
- C. L. Hill, in *Comprehensive Coordination Chemistry II*, ed. J. A. McLverty and T. J. Meyer, Elsevier, Amsterdam, 2004, vol. 4, p. 679.
- K.-F. Aguey-Zinsou, P. V. Bernhardt, U. Kappler and A. G. McEwan, *J. Am. Chem. Soc.*, 2003, **125**, 530–535.
- D. A. Judd, J. H. Nettles, N. Nevins, J. P. Snyder, D. C. Liotta, J. Tang, J. Ermoloeff, R. F. Schinazi and C. L. Hill, *J. Am. Chem. Soc.*, 2001, **123**, 886–897.
- B. Hasenknopf, *Front. Biosci.*, 2005, **10**, 275–287.
- H. Zeng, G. R. Newkome and C. L. Hill, *Angew. Chem., Int. Ed.*, 2000, **39**, 1772–1774.
- M. T. Pope and A. Mueller, *Angew. Chem., Int. Ed. Engl.*, 1991, **103**, 56–70.
- F. Ogliaro, S. P. de Visser, S. Cohen, P. K. Sharma and S. Shaik, *J. Am. Chem. Soc.*, 2002, **124**, 2806–2817.

- 12 T. R. Zhang, W. Feng, R. Lu, C. Y. Bao, T. J. Li, Y. Y. Zhao and J. N. Yao, *J. Solid State Chem.*, 2002, **166**, 259–263.
- 13 T. Yamase, *Chem. Rev.*, 1998, **98**, 307–325.
- 14 D. Long, E. Burkholder and L. Cronin, *Chem. Soc. Rev.*, 2007, **36**, 105.
- 15 B. Dawson, *Acta Crystallogr.*, 1953, **6**, 113–126.
- 16 M. Holscher, U. Englert, B. Zibrowius and W. Holderich, *Angew. Chem., Int. Ed. Engl.*, 1994, **106**, 2552–2554.
- 17 H. Ichida and Y. Sasaki, *Acta Crystallogr., Sect. C: Cryst. Struct. Commun.*, 1983, **C39**, 529–533.
- 18 R. Neier, C. Trojanowski and R. Mattes, *J. Chem. Soc., Dalton Trans.*, 1995, 2521–2528.
- 19 P. J. S. Richardt, R. W. Gable, A. M. Bond and A. G. Wedd, *Inorg. Chem.*, 2001, **40**, 703–709.
- 20 D. M. Way, J. B. Cooper, M. Sadek, T. Vu, P. J. Mahon, A. M. Bond, R. T. C. Brownlee and A. G. Wedd, *Inorg. Chem.*, 1997, **36**, 4227–4233.
- 21 S. Zhu, B. Yue, X. Shi, Y. Gu, J. Liu, M. Chen and Y. Huang, *J. Chem. Soc., Dalton Trans.*, 1993, 3633–3634.
- 22 F. H. Herbstein and R. E. Marsh, *Acta Crystallogr., Sect. B*, 1998, **B54**, 677–686.
- 23 D.-L. Long, P. Kögerler and L. Cronin, *Angew. Chem., Int. Ed.*, 2004, **43**, 1817–1820.
- 24 C. Baffert, J. F. Boas, A. M. Bond, P. Kögerler, D.-L. Long, T. W. Pilbrow and L. Cronin, *Chem.–Eur. J.*, 2006, **12**, 8472–8483.
- 25 E. Papaconstantinou and M. T. Pope, *Inorg. Chem.*, 1967, **6**, 1152–1155.
- 26 A. M. Bond, *Broadening Electrochemical Horizons*, Oxford University Press, Oxford, 2002, chapter 2 and references therein.
- 27 *CRC Handbook of Chemistry and Physics*, 85th edn, 2004, .
- 28 A. J. Bard and L. R. Faulkner, *Electrochemical Methods: Fundamentals and Applications*, John Wiley and Sons, New York, 2nd edn, 2001.
- 29 H. M. Koepp, H. Wendt and H. Z. Strehlow, *Z. Elektrochem.*, 1960, **64**, 483.
- 30 F. Scholz and B. Meyer, *Electroanal. Chem.*, 1998, **20**, 1–86.
- 31 S.-X. Guo, S. W. Feldberg, A. M. Bond, D. L. Callahan, P. J. S. Richardt and A. G. Wedd, *J. Phys. Chem. B*, 2005, **109**, 20641–20651.
- 32 G. Balducci and G. Costa, *J. Electroanal. Chem.*, 1993, **348**, 355–365.
- 33 S. Hee Hong, D. H. Evans, S. F. Nelsen and R. F. Ismagilov, *J. Electroanal. Chem.*, 2000, **486**, 75–84.
- 34 M. A. Zon, N. C. Marchiando and H. Fernandez, *J. Electroanal. Chem.*, 1999, **465**, 225–233.
- 35 J. Jacq, *J. Electroanal. Chem.*, 1971, **29**, 149–180.
- 36 E. Laviron, A. Vallat and R. Meunier-Prest, *J. Electroanal. Chem.*, 1994, **379**, 427–435.
- 37 (a) E. Laviron, *J. Electroanal. Chem.*, 1980, **109**, 57–67; (b) E. Laviron, *J. Electroanal. Chem.*, 1981, **130**, 23–29; (c) E. Laviron, *J. Electroanal. Chem.*, 1981, **124**, 1–7; (d) E. Laviron, *J. Electroanal. Chem.*, 1982, **137**, 1–15; (e) E. Laviron, *J. Electroanal. Chem.*, 1983, **146**, 15–36; (f) E. Laviron, *J. Electroanal. Chem.*, 1983, **146**, 1–13; (g) E. Laviron, *J. Electroanal. Chem.*, 1984, **164**, 213–227; (h) E. Laviron, *J. Electroanal. Chem.*, 1984, **169**, 29–46.
- 38 E. Laviron and L. Roullier, *J. Electroanal. Chem.*, 1990, **288**, 165–175.
- 39 E. Laviron and R. Meunier-Prest, *J. Electroanal. Chem.*, 1992, **324**, 1–18.
- 40 E. Laviron, R. Meunier-Prest and R. Lacasse, *J. Electroanal. Chem.*, 1994, **375**, 263–274.
- 41 (a) M. Seralathan and S. K. Rangarajan, *J. Electroanal. Chem.*, 1985, **191**, 229–235; (b) M. Seralathan and S. K. Rangarajan, *J. Electroanal. Chem.*, 1985, **191**, 237–252; (c) M. Seralathan and S. K. Rangarajan, *J. Electroanal. Chem.*, 1985, **191**, 209–228.
- 42 M. Rueda, I. Navarro, F. Prieto, M. Sluyters-Rehbach and J. H. Sluyters, *J. Electroanal. Chem.*, 1994, **371**, 179–189.
- 43 E. T. Smith, *Curr. Sep.*, 2004, **21**, 11–13.
- 44 C. F. Gonzalez-Fernandez, M. T. Garcia-Hernandez and J. Horno, *J. Electroanal. Chem.*, 1995, **395**, 39–44.
- 45 M. Salas, B. Gordillo and F. J. Gonzalez, *J. Electroanal. Chem.*, 2004, **574**, 33–39.
- 46 M. T. Garcia-Hernandez, J. Castilla, C. F. Gonzalez-Fernandez and J. Horno, *J. Electroanal. Chem.*, 1997, **424**, 207–212.
- 47 J. Zhang, A. M. Bond, P. J. S. Richardt and A. G. Wedd, *Inorg. Chem.*, 2004, **43**, 8263–8271.
- 48 D. M. Way, A. M. Bond and A. G. Wedd, *Inorg. Chem.*, 1997, **36**, 2826–2833.
- 49 J. N. Barrows and M. T. Pope, *Inorg. Chim. Acta*, 1993, **213**, 91–98.